

Liquid-Crystalline Phase Transition in Organophosphazenes

Keiichi Moriya,^{1*} Toshiya Suzuki,¹ Yasuyuki Kawanishi,¹ Tsuyoshi Masuda,¹ Hiroshi Mizusaki,¹ Shigekazu Nakagawa,¹ Hiroshi Ikematsu,¹ Katsuyuki Mizuno,¹ Shinichi Yano¹ and Meisetsu Kajiwara²

¹Department of Chemistry, Faculty of Engineering, Gifu University, Yanagido, Gifu 501-1193, Japan

²School of Dentistry, Aichigakuin University, Kusumoto-cho, 1-100, Chikusa-ku, 464-8586, Japan

Organophosphazenes with a similar mesogenic moiety were prepared and their mesogenicity was studied by differential scanning calorimetry (DSC) measurements and polarizing microscope observations. In cyclotriphosphazenes with alkoxybiphenyl and Schiff base moieties, mesomorphic phase transitions were observed, but no mesomorphic phase was observed for the corresponding cyclotetraphosphazenes. In polyphosphazenes with an alkoxybiphenyl moiety, no mesomorphic phase was observed. The molecular structure of cyclotriphosphazenes facilitated the formation of a mesomorphic layer structure; in contrast, the formation of a mesomorphic layer structure did not occur in cyclotetraphosphazenes and polyphosphazenes, even though they bore a similar mesogenic moiety. Moreover, in cyclotriphosphazenes with an optically active alkoxybiphenyl group, a smectic C* phase was observed. The spontaneous polarization of the compound was $-190 \mu \text{C m}^{-2}$ at 436 K in 25 μ in cell using the triangular-wave method. © 1998 John Wiley & Sons, Ltd.

Keywords: organophosphazenes; liquid crystals; phase transition

Received 21 October 1997; accepted 11 February 1998

INTRODUCTION

Much attention has been focused on organophosphazenes because they consist of inorganic backbones as well as organic side-chains. Thus they can be considered as hybrids of organic and inorganic compounds and their properties are a combination

of both. The functional properties of polymers and trimers consisting of organophosphazenes have been studied extensively.^{1–5}

Several liquid-crystalline organophosphazenes including polymers and trimers have been synthesized but their structural features seem to lie in the long alkyl-ether chains between the mesogenic side-groups and the phosphazene backbones.^{6–10} We considered that the direct introduction of aryloxy mesogenic side-groups into the organophosphazene backbones (the P=N linkages) without any spacer could produce interesting properties because the movement of the mesogens is limited by the linkage between mesogenic side-chains and the organophosphazene backbones. Hence, we tried to introduce aryloxy mesogenic side-groups directly to the organophosphazene backbones without any spacer, and we studied their phase transition and mesogenicity using thermal, optical and spectroscopic methods to see how their mesogenicity would be changed in these multi-substituted phosphazene nuclei. These compounds make an interesting group of liquid crystals because of their peculiar molecular shape.^{11–18}

In this paper, we describe the liquid-crystalline phase transition of cyclotriphosphazenes, cyclotetraphosphazenes and polyphosphazene bearing similar mesogenic groups. We also describe the relationship between molecular structure and mesogenicity. The chemical structures of the organophosphazenes studied are shown in Fig. 1.

EXPERIMENTAL

Reactions were monitored by thin-layer chromatography (TLC) using Merck 60 F₂₅₄ precoated silica-gel plates (thickness 0.25 mm). Silica gel (Wakogel C-200) and reagent-grade solvents were used for column chromatography. All substrate analogues

* Correspondence to: K. Moriya, Department of Chemistry, Faculty of Engineering, Gifu University, Yanagido, Gifu 501-1193, Japan.

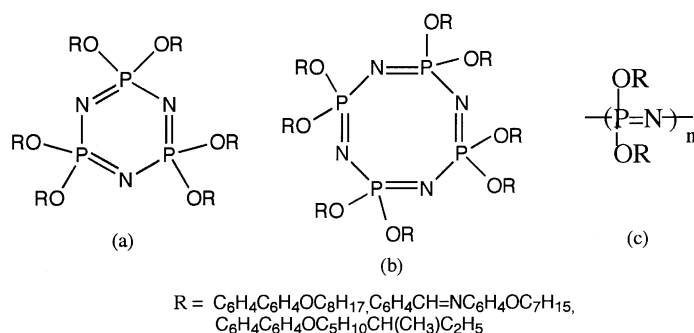


Figure 1 Chemical structure of organophosphazene (a) trimer, (b) tetramer and (c) polymer.

were purified chromatographically to homogeneity by TLC analysis and purity was confirmed by ¹H and ³¹P NMR. The solvent was distilled before use. All solvents are reagent-grade unless otherwise stated, and anhydrous solvents were dried immediately before use.

Synthesis of organophosphazenes with an alkoxybiphenyl moiety

4-Hydroxy-(4'-octyloxy)biphenyl (HOB) was prepared from 4,4'-dihydroxybiphenyl (80 g, 0.43 mol), 1-bromo-octane (55.2 g, 0.29 mol) and KOH (24.2 g, 0.43 mol) in ethanol (1200 ml) under reflux for 6 h. The crystals obtained were recrystallized from toluene and ethanol, once and twice respectively. The purity was examined by TLC (silica gel, chloroform).

Hexakis [4'-(4-octyloxy)biphenoxy]cyclotriposphazene (HOCP) was prepared by the reaction of hexachlorocyclotriposphazene (HCCP) (supplied by Nihon Fine Chemicals Co., Ltd) (2.6 g, 7 mmol), HOB (20 g, 67 mmol) and sodium hydride (1.6 g, 67 mmol) in dioxane solution (200 ml) in the presence of tetra-n-butylammonium bromide (1.3 g, 4 mmol).¹⁷ After the solution had been refluxed for 24 h, the crude products were purified using column chromatography (chloroform) and then recrystallized from 1:1 tetrahydrofuran (THF)/cyclohexane. The purified HOCP crystals were characterized by TLC (7:3, chloroform/hexane), IR, ¹H and ³¹P NMR, and elemental analyses. The analytical results for HOCP were as follows: m.p. 440 K, clearing point (c.p.) 457 K; IR (KBr) 2930, 1608, 1240, 1170, 980, 760 cm⁻¹; ¹H NMR (CDCl₃) δ 0.9 (t, 6.8 Hz, 6H), 1.3–1.8 (m, 13H), 4.4 (m, 1H), 6.8 (d, 8.4 Hz, 2H), 6.9 (d, 8.5 Hz, 2H), 7.2 (d, 8.4 Hz, 2H), 7.3 (d, 8.5 Hz, 2H); ³¹P NMR δ

10.6(s). Analysis: Calcd for C₁₂₀H₁₅₀N₃O₁₂P₃: C, 75.09; H, 7.88; N, 2.19; found: C, 74.93; H, 7.96; N, 2.23%.

The synthesis of 4-hydroxy (4'-octyloxy)biphenyl (HOB) was described above. Octakis-[4'-(4-octyloxy)biphenoxy]cyclooctaphosphazene (OOCOP) was prepared by the reaction of octachlorocyclooctaphosphazene (3.48 g, 7.5 mmol) (supplied by Nihon Soda Co., Ltd), HOB (19.8 g, 60.0 mmol) and sodium hydride (2.40 g, 60.0 mmol) in the presence of tetra-n-butylammonium bromide (1.93 g, 60 mmol) in dioxane (200 ml) under reflux for 26 h. The crude crystals obtained were purified by recrystallizing from 3:20 THF/cyclohexane after column chromatography (CHCl₃). OOCOP was confirmed to be thoroughly purified on the basis of NMR and IR spectra. The analytical results for OOCOP were as follows: m.p. 411 K; IR (KBr) 2925, 1607, 1493, 1244, 1169, 966, 725 cm⁻¹; ¹H NMR (CDCl₃) δ 0.9(t, 6.8 Hz, 3H), 1.30–1.83(m, 12H), 3.96 (t, 7.3 Hz, 2H), 6.82–7.30 (m, 8H), 6.9 (d, 8.5 Hz, 2H), 7.2 (d, 8.4 Hz, 2H), 7.3 (d, 8.5 Hz, 2H); ³¹P NMR δ -11.1(s).

Polydichlorophosphazene (PDCP) was prepared from the ring-opening polymerization of hexachlorocyclotriposphazene (20 g, 58 mmol) using sulfur (0.32 g, 10 mmol) as a catalyst at 270 °C for 3 h in an evacuated pyrex tube.

Poly {bis[4'-(4-octyloxy)biphenoxy]phosphazene} (POP) was prepared by the substitution reaction of PDCP (0.98 g, 8.5 mmol) and 4-hydroxy (4'-octyloxy)biphenyl (10.7 g, 35 mmol) and NaH (0.84 g, 35 mmol) in the presence of tetra-n-butylammonium bromide (1.1 g, 3.5 mmol) in THF (50 ml) under reflux for 160 h. The reaction was followed by ³¹P NMR. The obtained polymers were extracted by Soxhlet apparatus using THF/ethanol (1:1) solution after the THF solution of the

polymer was reprecipitated into ethanol. The ^{31}P NMR showed a broad singlet around -14 ppm but the elemental analysis confirmed that only 66% of the side-chains were attached to the polyphosphazenes.

Synthesis of organophosphazenes with a Schiff base moiety

4-Heptyloxyacetanilide was synthesized from 4-hydroxyacetanilide (25 g, 0.16 mol), bromoheptane (28.5 g, 0.16 mol) and KOH (11 g, 0.17 mol) in ethanol (200 ml) under reflux for 6 h. The crude products obtained were recrystallized three times from 1:3 water ethanol mixed solvent. The purity of the sample was determined by TLC (ethyl acetate). 4-Heptyloxyaniline was synthesized from 4-heptyloxyacetanilide (20 g, 83 mmol) and KOH (15 g, 0.23 mol) in ethanol (200 ml) under reflux for 24 h. After the reaction was finished, the solution was added to water (50 ml). The crude products were extracted with benzene and then recrystallized four times from 3:1 water ethanol solution. The purity of the sample was recognized by TLC (ethyl acetate). Hexakis(4-formylphenoxy)cyclotriphosphazene was synthesized from 4-hydroxybenzaldehyde (30.2 g, 0.25 mol), NaH (6.0 g, 0.25 mol) and hexachlorocyclotriphosphazene (12.1 g, 34 mmol) in THF (200 ml) under reflux for 2 h. The crude products were recrystallized from hexane THF solution. The product was confirmed by TLC (ethyl acetate), ^1H and ^{31}P NMR.

Hexakis{[4-[*N*-(4'-heptyloxyphenyl)iminomethyl]phenoxy]} cyclotriphosphazene (HHICP) was prepared by the reaction of hexakis(4-formylphenoxy)cyclotriphosphazene (1.06 g, 1.2 mmol) and 4-heptyloxyaniline (2.48 g, 12 mmol) in benzene (100 ml) under reflux for 6 h. The crude products obtained were recrystallized three times from absolute THF after separation by filtration. The products were judged to be thoroughly purified by ^1H and ^{31}P NMR, and elemental analysis. The analytical results for HHICP were as follows. m.p. 463 K, c.p. 515 K; IR (KBr) 2933, 2858, 1626, 1604, 1578, 1251, 1219, 1161, 983 cm^{-1} ; ^1H NMR (CDCl_3) δ 1.1 (t, 7.3 Hz, 6H), 1.3–1.8 (m, 10H), 3.9 (t, 7.3 Hz, 2H), 6.8 (d, 8.8 Hz, 2H), 7.0 (d, 8.8 Hz, 2H), 7.1 (d, 8.8 Hz, 2H), 7.7 (d, 8.45 Hz, 2H), 8.4 (s, 1H); ^{31}P NMR δ 9.7(s). Analysis: Calcd for $\text{C}_{120}\text{H}_{144}\text{N}_9\text{O}_{12}\text{P}_3$: C, 72.16; H, 7.27; N, 6.31; found: C, 71.76; H, 7.21; N, 6.28%.

The syntheses of 4-heptyloxyaniline and 4-heptyloxyacetanilide were described above. Hexakis(4-formylphenoxy)cyclotetraphosphazene was

synthesized from 4-hydroxybenzaldehyde (17.5 g, 0.143 mol), NaH (5.73 g, 0.143 mol) and hexachlorocyclotetraphosphazene (5.0 g, 10.6 mmol) in THF (125 ml) under reflux for 2 h. The crude products were purified by reprecipitation in hexane after being dissolved in a small amount of THF. The product was confirmed by TLC (1:1 ethyl acetate chloroform) and ^1H and ^{31}P NMR.

Octakis{[4-[*N*-(4'-heptyloxyphenyl)iminomethyl]phenoxy]} cyclotetraphosphazene (OHICP) was prepared by the reaction of hexakis(4-formylphenoxy)cyclotetraphosphazene (1.0 g, 0.87 mmol) and 4-heptyloxyaniline (2.7 g, 13 mmol) in benzene (50 ml) under reflux for 6 h. Water present in the solution was removed by the molecular sieves in the Dean–Stark tube. The crude products obtained were recrystallized three times from benzene and once from 1:1 THF cyclohexane after being separated by filtration. The products were characterized by ^1H and ^{31}P NMR. The analytical results for OHICP were as follows: m.p. 425 K; IR (KBr) 2933, 2858, 1604, 1578, 1251, 1219, 1161, 983 cm^{-1} ; ^1H NMR (CDCl_3) δ 1.1(t, 7.3 Hz, 3H), 1.3–1.8 (m, 10H), 3.9 (t, 7.3 Hz, 2H), 6.8 (d, 8.8 Hz, 2H), 7.0 (d, 8.8 Hz, 2H), 7.3 (d, 8.4 Hz, 2H), 8.4 (s, 1H); ^{31}P NMR δ -12.7 (s).

Synthesis of a cyclotriphosphazene with an optically active alkoxybiphenyl moiety

(*S*)-Hexakis{[4-[4'-6-methyloctyloxy]biphenoxy]} cyclotriphosphazene (SMOCP) was synthesized using the following procedure. (*S*)-1-Chloro-2-methylbutane (SCMB) ($[\alpha]^{25} = -4.6^\circ$) was prepared from (*S*)-2-methylbutanol (41 g, 0.47 mol, $[\alpha]^{25} = -5.8^\circ$) according to the described procedures.¹⁹ A suspension of 1,4-dibromoethane (26 g, 0.12 mol) and dilithium tetrachlorocuprate (0.42 g, 1.9 mmol) in THF (100 ml) was added to the Grignard reagent prepared from SCMB (20 g, 0.19 mol) and Mg (4.6 g, 0.19 mol) in diethyl ether (100 ml).^{20–23} The dilithium tetrachlorocuprate was obtained by the reaction of lithium chloride (0.16 g, 3.8 mmol) and cupric chloride (0.26 g, 1.9 mmol) in THF (40 ml). The mixture was gradually warmed to ambient temperature over the course of 4 h with stirring. After a further 24 h, distillation of the crude product under 8 mmHg gave 12.3 g of (*S*)-1-bromo-6-methyloctane (SBM) with $[\alpha]^{25} = +7.7^\circ\text{C}$. (*S*)-4-(6-Methyloctyloxy)biphenyl-4'-ol (SMBO) was prepared by heating a mixture of SBM (12 g, 58 mmol), 4,4'-dihydroxybiphenyl (16 g, 87 mmol) and potassium hydroxide (5.9 g,

90 mmol) in ethanol (500 ml) under reflux for 8 h. The crude product, when filtered using hot toluene, crystallized out from the filtrate upon cooling to room temperature. The crystals obtained were purified by column chromatography (CHCl_3), followed by recrystallization from hexane; m.p. 405 K, $[\alpha]^{25} = +7.3^\circ$.

The sodium salt of SMBO (10 g, 32 mmol), prepared by treating with NaH (1.4 g, 35 mmol) in dioxane (25 ml), was mixed with hexachlorocyclotriphosphazene (HCCP) (1.6 g, 4.4 mmol) and tetra-*n*-butylammonium bromide (1.0 g, 3.2 mmol) in dioxane (45 ml). The solution was heated under reflux for 24 h. The crude SMOCP product was subjected to column chromatography (CHCl_3) and recrystallized from hexane/THF (20 : 1). The analytical results for SMOCP were as follows: m.p. 418 K, c.p. 441 K; $[\alpha]^{27} = +5.9^\circ$ (*c* 1.0, CHCl_3); IR (KBr): 2930, 1608–1497, 1249, 1166, 963, 730 cm^{-1} ; ^1H NMR (CDCl_3) δ 0.9 (m, 6H), 1.1–1.5 (m, 9H), 1.8 (m, 2H), 4.0 (t, 6.6 Hz, 2H), 6.8 (d, 8.4 Hz, 2H), 6.9 (d, 8.4 Hz, 2H), 7.2 (d, 8.8 Hz, 2H), 7.4 (d, 8.4 Hz, 2H); ^{31}P NMR δ 10.6 (s). Analysis: Calcd for $\text{C}_{126}\text{H}_{162}\text{N}_3\text{O}_{12}\text{P}_3$: C, 75.53; H, 8.15; N, 2.10; found: C, 75.83; H, 8.30; N, 2.10%.

1-Bromo-6-methyloctane (MO) was prepared from the Grignard reagent from 1-chloro-2-methylbutane, and 1,4-dibromoethane, in the presence of dilithium tetrachlorocuprate in THF solution. 4-(6-Methyloctyloxy)biphenyl-4'-ol (MOBP) was synthesized from MO and 4,4'-dihydroxybiphenyl. The racemic mixture of hexakis {[4-(4'-6-methyloctyloxy)biphenoxy]} cyclotriphosphazene (MOCP) was prepared from HCCP and MOBP using a method similar to that for SMOCP and judged to be thoroughly purified by the same method.

Analytical techniques and instruments

Phase transition temperatures were measured using a differential scanning calorimeter (Seiko Electronics DSC 210) and texture observations were performed using an optical polarizing microscope (Nikon Optiphot-pol XTP-11) equipped with a Mettler FP 82 hot stage at a heating/cooling rate of 5 K min^{-1} from room temperature up to above the melting or clearing point. ^1H NMR (solvent CDCl_3) and ^{31}P NMR (solvent THF) were recorded on a JEOL JNM-GX 270 spectrometer using TMS as the internal standard for the former and 85% H_3PO_4 as the external standard for the latter. The lock signal for ^{31}P NMR was provided by external D_2O inserts.

The optical purity of the chiral compounds was determined by measurement of optical rotatory power, using an atomic digital polarizer (Otsuka Electronics Co. Ltd; PM-201A). Spontaneous polarization was measured by the triangular-wave method^{24,25} using a wave-function generator (NF Electronic Instruments, 1920A) and an amplifier (NF Electronic Instruments, 4005) and simultaneously observing the texture of the sample with a polarizing microscope (Nikon Optiphot-pol XTP-11) by cooling from an isotropic liquid at a rate of 0.1 K min^{-1} . The triangular wave applied was 1 Hz and 150 V. Signals of the samples were read by a digital oscilloscope (Hitachi VC-6020) and transferred to a microcomputer (NEC, PC9801). The apparatus was calibrated by measuring the spontaneous polarization of (*S*)-2-methylbutyl 4-(4'-decyloxybenzylideneamino)cinnamate (DOBAMBC). The spontaneous polarization for DOBAMBC is 8.15 $\mu\text{C m}^{-2}$ at 362 K, which is consistent with the value in the literature.^{26,27} The measurements were performed on a 1.4, 3.7, 12 and 25 μm -thick antiparallel-oriented liquid-crystalline cell, whose sample area is confined to 20 mm^2 by etching the ITO-coated glass surfaces. The antiparallel orientation^{28–30} was obtained by rubbing with a velvet cloth using a handmade rubbing machine after coating with polyimide, PSI-A-X044-CF1 (Chisso Petrochemical Co.). For an accurate calculation of the spontaneous polarizations of the SMOCP, a separately synthesized racemic mixture of MOCP was used as the base line of the signal. The tilt angles were measured by the angles between the two distinction positions, which are determined by applying a DC electric field of sufficient strength to release the helix of the ferroelectric liquid crystals in the smectic C* layer perpendicular to the substrate liquid-crystalline cells.

RESULTS AND DISCUSSION

Mesogenicity of organophosphazenes with a 4-octyloxybiphenoxy moiety

In this section hexakis [4'-(4-octyloxy)biphenoxy]cyclotriphosphazene (HOCP), octakis[4'-(4-octyloxy)biphenoxy]cyclotetraphosphazene (OOCp) and poly{bis[4'-(4-octyloxy)biphenoxy]phosphazene} (POP) will be described.

DSC thermograms of HOCP and OOCp for the first cooling process and the second heating process

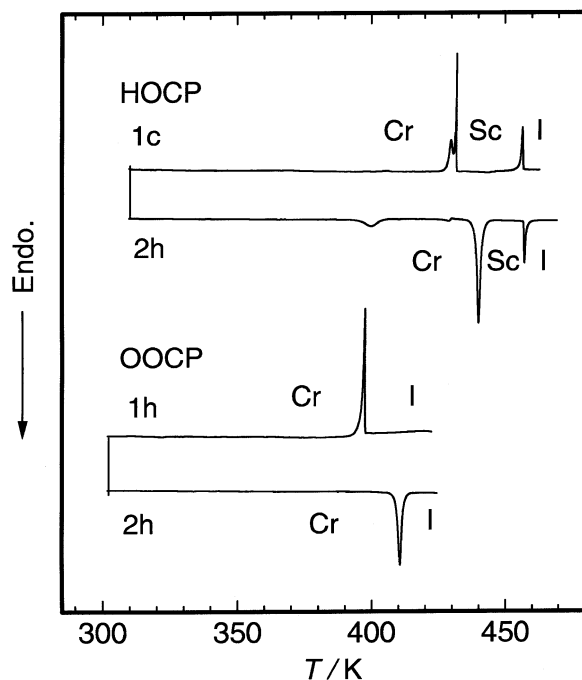


Figure 2 DSC thermograms of hexakis [4'-(4-octyloxy)biphenoxy]cyclotriphosphazene (HOCP) and octakis [4'-(4-octyloxy)biphenoxy]cyclotetraphosphazene (OOCp).

are shown in Fig. 2. In the first HOCP cooling process, three exothermic peaks are seen at 457, 432 and 430 K. In the second heating process, three endothermic peaks are seen at 400, 440 and 457 K. From the polarizing microscope observations, a schlieren texture with disclination lines having $s = \pm 1$ and a simultaneous broken-fan texture was observed between 457 and 432 K upon cooling from an isotropic liquid. This texture shows the existence of a smectic C phase.³¹ The thermal anomalies at 430 K in the first cooling process and at 400 K in the second heating process may correspond to crystal-crystal phase transitions because no other mesogenic texture was observed

in the polarizing microscope observations in these temperature regions. In the DSC thermograms of OOCp, only one exothermic peak, which corresponds to the phase transition from an isotropic liquid (I) to crystal (Cr), was observed at 397 K for the first cooling process. In the second heating process, only one endothermic peak, which corresponds to the Cr-I phase transition, was observed at 411 K. Using polarizing microscopy, no liquid-crystalline phase was observed for OOCp. The thermodynamic parameters of HOCP and OOCp obtained from the second heating process of the DSC measurements are shown in Table 1. It is found from Table 1 that the disorder of the SmC phase in HOCP is much closer to that in the isotropic liquid than to that in the crystal because the entropy change of the SmC-I phase transition ($\Delta S_{\text{SmC-I}}$) is much smaller than the melting entropy (ΔS_{m}) of HOCP.

In the X-ray single-crystal structure analysis of hexakis(4-biphenoxy)cyclotriphosphazene (HBCP) and octakis(4-biphenoxy)cyclotetraphosphazene (OBCP), the side-chains line up relatively regularly for the former and randomly for the latter.³² The molecular structure of the HOCP under the assumption of a similar situation in HBCP is shown in Fig. 3. The results of the mesogenic properties in HOCP and OOCp were interpreted as follows. The molecular organization of HOCP (trimer) helps the formation of the smectic layer structure because the ordering of the side-chains in HOCP increases the aspect ratio (the ratio of the molecular long axis to the short axis) of the molecule. However, the random orientation of the side chains in OOCp (tetramer) prevents the formation of the smectic layer structure.

For the polyphosphazenes with a similar alkoxy-biphenyl moiety (POP), only 66% of the side-chains were introduced in the 160 h-reaction sample, which was determined by elementary analysis. No liquid-crystalline phase transition in POP was observed by polarizing microscopy. This result suggests that the fully substituted poly-

Table 1 Thermodynamic parameters of hexakis [4'-(4-octyloxy)biphenoxy]cyclotriphosphazene (HOCP) and octakis [4'-(4-octyloxy)biphenoxy]cyclotetraphosphazene (OOCp) in the second heating process

Compound	T_{m} K	ΔS_{m} $\text{JK}^{-1}\text{mol}^{-1}$	$T_{\text{SmC-I}}$ K	$\Delta S_{\text{SmC-I}}$ $\text{JK}^{-1}\text{mol}^{-1}$
HOCP	440	184	457	33
OOCp	411	185		

T_{m} ; melting temperature, ΔS_{m} ; melting entropy, $T_{\text{SmC-I}}$; transition temperature from SmC to isotropic liquid, $\Delta S_{\text{SmC-I}}$; transition entropy from SmC to isotropic liquid.

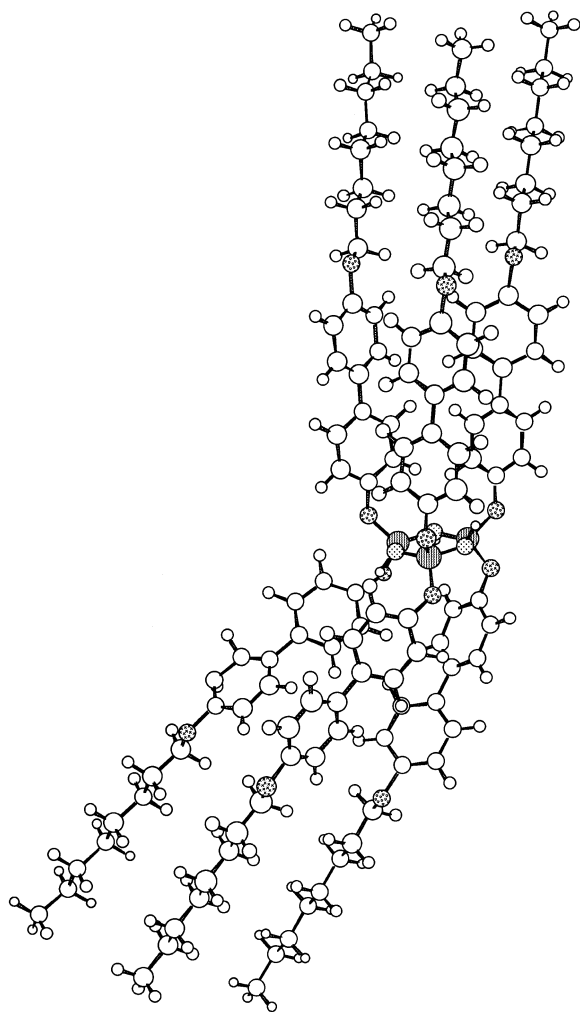


Figure 3 Assumed molecular structure of HOCP.

phosphazene with 4-octyloxybiphenyl side-groups cannot be prepared at atmospheric pressure and at the boiling temperature of THF.

Mesogenicity of organophosphazenes with a Schiff base moiety

The DSC thermograms of hexakis{4-[*N*-(4'-heptyloxyphenyl)iminomethyl]phenoxy}cyclotriphosphazene (HHICP) (trimer) and octakis{4-[*N*-(4'-heptyloxyphenyl)iminomethyl]phenoxy}cyclotetraphosphazene (OHICP) (tetramer) are shown in Fig. 4. In the first HHICP cooling process, two large and two small exothermic peaks are seen at 514 and 457 K, and at 503 and 486 K, respectively. From

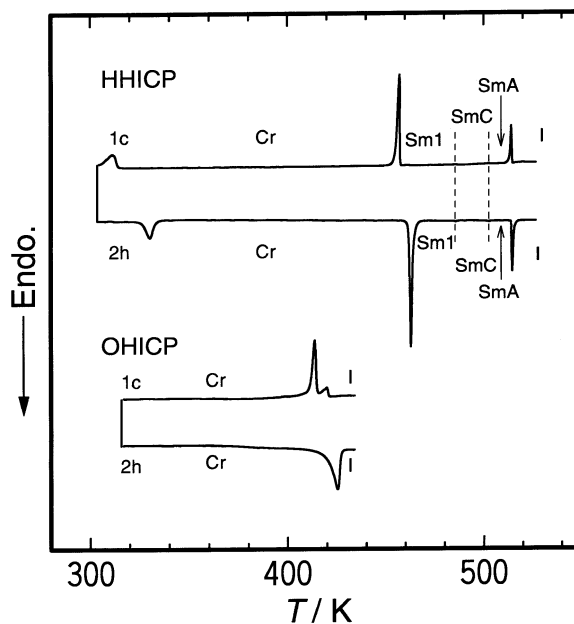


Figure 4 DSC thermograms of hexakis {4-[*N*-(4'-heptyloxyphenyl)iminomethyl]phenoxy}cyclotriphosphazene (HHICP) and octakis {4-[*N*-(4'-heptyloxyphenyl)iminomethyl]phenoxy}cyclotetraphosphazene (OHICP).

the polarizing microscope observations, the peaks at 514 and 457 K correspond to the clearing and freezing point. Upon cooling from an isotropic liquid, an SmA phase with fan and black (homeotropic) textures was observed at 514 K. Below 503 K, the fan and black textures changed to broken-fan and simultaneous schlieren texture with disclination lines having $s = \pm 1$, showing the presence of the SmC. Below 486 K, the schlieren texture changed to a mosaic one during the cooling process. This phase is a more ordered smectic phase than that of smectic C but was not determined. For the identification of this phase, a more precise experiment, e.g. a mixing test with a liquid crystal of known phases will be needed. At 457 K, the mesomorphic phase changed to a crystal. In the second HHICP heating process (Fig. 4), five endothermic peaks are seen in the DSC thermograms at 330, 463, 486, 503 and 515 K. The endothermic peaks at 463 and 515 K from the polarizing microscope observations correspond to melting and clearing points, respectively. The small peaks at 486 and 503 K are considered to correspond to the Sm1–SmC and SmC–SmA phase transitions because the phase-transition temperatures and phase-transition entropies are similar to

Table 2 The thermodynamic parameters of hexakis {4-[N-(4'-heptyloxyphenyl)iminomethyl]phenoxy}cyclotriphosphazene (HHICP) and octakis {4-[N-(4'-heptyloxyphenyl)iminomethyl]phenoxy}cyclotetraphosphazene (OHICP) in the second heating process

Compound	T_m K	$\frac{\Delta S_m}{JK^{-1}mol^{-1}}$	T_{S1-SmC} K	$\frac{\Delta S_{S1-SmC}}{JK^{-1}mol^{-1}}$	$T_{SmC-SmA}$ K	$\frac{\Delta S_{SmC-SmA}}{JK^{-1}mol^{-1}}$	T_{SmA-I} K	$\frac{\Delta S_{SmA-I}}{JK^{-1}mol^{-1}}$
HHICP	463	166	486	0.7	503	0.4	515	33
OHICP	425	191						

T_m : melting temperature, ΔS_m : melting entropy, T_{S1-SmC} : S1-SmC transition temperature, ΔS_{S1-SmC} : S1-SmC transition entropy, $T_{SmC-SmA}$: SmC-SmA transition temperature, $\Delta S_{SmC-SmA}$: SmC-SmA transition entropy, T_{SmA-I} : transition temperature from SmA to isotropic liquid, ΔS_{SmA-I} : transition entropy from SmA to isotropic liquid.

those of the first cooling process. The thermodynamic parameters obtained from DSC measurements of the second heating process are shown in Table 2 along with those of the tetrameric derivative (OHICP). The low entropies of the Sm1-SmC and SmC-SmA phase transitions suggest that the structures of the Sm1, SmC and SmA phases are very close together.

In the first cooling process in the DSC thermograms of OHICP (Fig. 4), two exothermic peaks are seen around 420 and 414 K. Between the two exothermic peaks, the existence of a mesomorphic phase can be expected. However, the polarizing microscope observation did not reveal a clear mesomorphic texture. In the second OHICP heating process, only one endothermic phase corresponding to melting is seen at 425 K; in addition, no mesomorphic phase was observed by polarizing microscopy.

Mesogenicity of a cyclotriphosphazene with an optically active moiety

A chiral moiety was introduced into the alkoxy groups of the side-chains and their mesogenicity was studied. The DSC thermograms of (*S*)-hexakis{4-[4'-(6-methyl)octyloxy]biphenoxy}cyclotriphosphazene (SMOCP) (trimer) are shown in Fig. 5. In the first SMOCP cooling process, three exothermic peaks were observed at 440, 403 and 352 K. Polarizing microscopy showed a shlieren texture with disclination lines having $s = \pm 1$ and a simultaneous broken-fan texture with a stripe between 440 and 403 K. This demonstrates the existence of a smectic C* phase. The SMOCP changed to a crystal at 403 K on the polarizing microscope. In the second heating of SMOCP, three endothermic peaks were observed at 410, 418 and 441 K. From the polarizing microscope observation, the peak at 418 K corresponds to the melting point. The thermodynamic parameters of SMOCP

obtained from the second heating process b, DSC measurements are shown in Table 3. The first-order nature of the phase transition is detected by the DSC measurements in which the entropy of the SmC-I phase transition is relatively large ($\Delta S \approx 28 JK^{-1} mol^{-1}$). The values of the transition entropy are much larger than those of the usual liquid crystals, consisting of rigid central groups and flexible end-groups.

The width of the stripe in the broken-fan texture in the homogeneous cell, in which the smectic layer is almost perpendicular to the glass slide, shows helical pitches in the Sc* phase. The helical pitches are about 12 μm at 436 K. This large value suggests that the twisting power of SMOCP in the Sc* phase is relatively small. The dependence of the liquid-crystalline cell thickness on the spontaneous polarization observed for the cell thicknesses of 1.4, 3.7, 12 and 25 μm is seen in Fig. 6 in which T_c is 440 K. The spontaneous polarization is -71, -110, -150 and -190 $\mu C m^{-2}$ for cell thicknesses

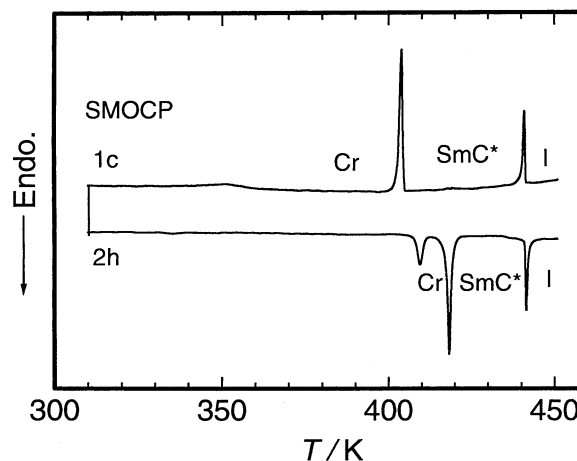
**Figure 5** DSC thermograms of (*S*)-hexakis {4-[4'-(6-methyl)octyloxy]biphenoxy}cyclotriphosphazene (SMOCP).

Table 3 The thermodynamic parameters of hexakis {4-[4'-((S)6-methyl)octyloxy]biphenoxy} cyclotriphosphazene (SMOCP) in the second heating process

Compound	T_m K	$\frac{\Delta S_m}{JK^{-1}mol^{-1}}$	$\frac{T_{SmC-I}}{K}$	$\frac{\Delta S_{SmC-I}}{JK^{-1}mol^{-1}}$
SMOCP	418	80	441	29

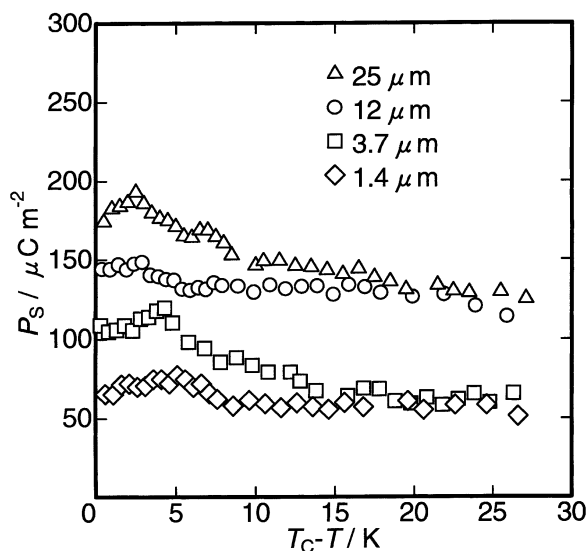
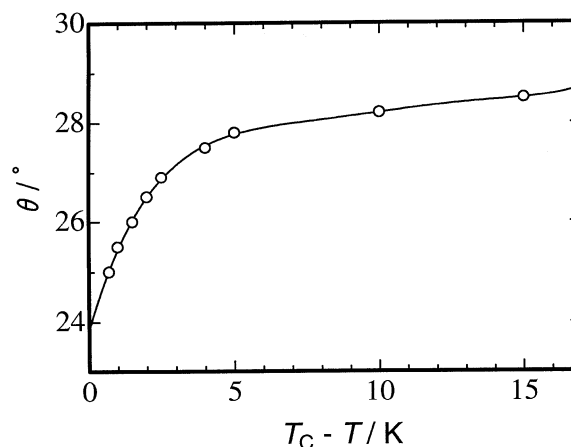
T_m ; melting temperature, ΔS_m ; entropy of melting, T_{SmC-I} ; transition temperature from SmC to isotropic liquid, ΔS_{SmC-I} ; transition entropy from SmC to isotropic liquid.

of 1.4, 3.7, 12 and 25 μm respectively, at 436 K. These values are several times larger than that of (S)-2-methylbutyl 4-(4'-decyloxybenzylidene)aminocinnamate (DOBAMBC). These relatively large values may be caused by the ether linkage of the alkoxy end-groups. The spontaneous polarization decreased with a decrease in the thickness of liquid crystalline cells. This is due to the cell surface effect at the interface between the liquid-crystalline cell (polyimide) and the liquid crystal (SMOCP). The surface effect seems to increase with decreasing cell thickness. For a 25 μm cell, decreasing temperature causes a spontaneous polarization increase and shows a maximum around $T_c - T = 2.5$ K. The maximum of the spontaneous polarization decreases slightly to lower temperature with decreasing cell thickness. The temperature dependences of the tilt angles are shown in Fig. 7. The tilt angle is ca 25° at T_c and increases with decreasing temperature. These results show that the phase transition of the isotropic liquid–Sc* phase

has a first-order characteristic. The tilt angle becomes 28° around $T - T_c = 6$ K and shows only a slight increase below this temperature.

CONCLUSIONS

Liquid crystalline phase transitions were studied using DSC measurements and polarizing microscopy. All cyclotriphosphazenes showed clear smectic phases. Interestingly, cyclotriphosphazene with an optically active side-group displayed a ferroelectric liquid-crystalline phase (Sc*) with a spontaneous polarization. On the other hand, the corresponding cyclotetraphosphazenes did not show a mesomorphic phase. From this result we can postulate that, in the cyclotriphosphazenes, each half of the mesogenic side-groups should extend perpendicularly upwards and downwards to the cyclotriphosphazene ring plane to facilitate the formation of the layer structure as in hexakis(4-biphenoxy)cyclotriphosphazene.¹⁴ The origin of the smectic architecture in the liquid-crystalline

**Figure 6** Dependence of cell thickness on the spontaneous polarization of Sc* in SMOCP.**Figure 7** Temperature dependence on the tilt angle in the Sc* phase of SMOCP.

phase is then attributable to these specific molecular frameworks. In contrast, in the cyclotetraphosphazenes the side-chains point in relatively random directions, thus preventing the formation of the layer structure. In the polymers, which are not fully substituted, no mesomorphic phase was observed. The polymer backbone of the polyphosphazenes may prevent the formation of the liquid-crystalline phase.

Acknowledgment We thank Nihon Soda Co. Ltd, the Japan Fine Chemicals, Co. Ltd and the Chisso Petrochemicals Co. for providing us with octachlorocyclotetraphosphazene, hexachlorocyclotriphosphazene and polyimide A-X044-CF1, respectively. We also express our thanks to Professors Hideo Takezoe and Yoichi Takanishi of the Tokyo Institute of Technology for teaching us the triangular-wave method techniques and for fruitful discussions.

REFERENCES

1. H. R. Allcock, *Chem. Rev.* **72**, 319 (1972).
2. H. R. Allcock, in: *Phosphorus-Nitrogen Compounds*, Academic Press, New York, 1972.
3. H. G. Heal, in: *The Inorganic Heterocyclic Chemistry of Sulphur, Nitrogen and Phosphorus*, Academic Press, New York, 1980, p. 214.
4. C. W. Allen, in: *The Chemistry of Inorganic Homo- and Heterocycles*, Vol. 2, Haiduc, I. and Sowerby, D. B. (eds), Academic Press, New York, 1987, p. 501.
5. C. W. Allen, *Organophosphorus Chem.* **21**, 368 (1990).
6. C. Kim and H. R. Allcock, *Macromolecules* **20**, 1726 (1987).
7. R. E. Singler, R. A. Willingham, R. W. Lenz, A. Furukawa and H. Finkellmann, *Macromolecules* **20**, 1727 (1987).
8. H. R. Allcock and C. Kim, *Macromolecules* **22**, 2596 (1989).
9. H. R. Allcock C. and C. Kim, *Macromolecules* **23**, 3881 (1990).
10. H. R. Allcock and E. H. Klingenberg, *Macromolecules* **28**, 4351 (1995).
11. K. Moriya, S. Yano and M. Kajiwara, *Chem. Lett.* 1039 (1990).
12. K. Moriya, S. Miyata, S. Yano and M. Kajiwara, *J. Inorg. Organomet. Polym.* **2**, 443 (1992).
13. K. Moriya, H. Mizusaki, M. Kato, S. Yano and M. Kajiwara, *Liq. Cryst.* **18**, 795 (1995).
14. K. Moriya, S. Nakagawa, S. Yano and M. Kajiwara, *Liq. Cryst.* **18**, 919 (1995).
15. K. Moriya, T. Suzuki, S. Yano and M. Kajiwara, *Liq. Cryst.* **19**, 711 (1995).
16. A. M. Levelut and K. Moriya, *Liq. Cryst.* **20**, 119 (1996).
17. K. Moriya, H. Mizusaki, M. Kato, T. Suzuki, S. Yano, M. Kajiwara and K. Tashiro, *Chem. Mater.* **9**, 255 (1997).
18. K. Moriya, T. Suzuki, H. Mizusaki, S. Yano and M. Kajiwara, *Chem. Lett.* 1001 (1997).
19. W. T. Bailey and E. T. Yates, *J. Org. Chem.* **26**, 3193 (1961).
20. B. Otterholm, M. Nilsson, S. T. Lagerwall and K. Skarp, *Liq. Cryst.* **2**, 757 (1987).
21. S. M. Kelly and K. Buchecker, *Helv. Chim. Acta* **71**, 451 (1988).
22. L. Friedman and A. Shani, *J. Am. Chem. Soc.* **96**, 7101 (1974).
23. M. Tamara and T. Kochi, *Synthesis* 303 (1971).
24. K. Miyasato, S. Abe, H. Takezoe, A. Fukuda and E. Kuze, *Jap. J. Appl. Phys.* **22**, L661 (1983).
25. H. Takezoe, K. Kondo, K. Miyasato, S. Abe, T. Tsuchiya, A. Fukuda and E. Kuze, *Ferroelectrics* **58**, 55 (1984).
26. S. Dumrongrattana and C. C. Huang, *Phys. Rev. Lett.* **56**, 464 (1986).
27. K. Kondo, H. Takezoe, A. Furukawa and E. Kuze, *Jpn. J. Appl. Phys.* **22**, L85 (1985).
28. K. Ishikawa, K. Hashimoto, H. Takezoe, A. Fukuda and E. Kuze, *Jpn. J. Appl. Phys.* **23**, L211 (1984).
29. K. Ishikawa, Y. Ouchi, T. Uemura, T. Tsuchiya, H. Takezoe and A. Fukuda, *Mol. Cryst. Liq. Cryst.* **122**, 175 (1985).
30. T. Hatano, K. Yamamoto, H. Takezoe and A. Fukuda, *Jpn. J. Appl. Phys.* **25**, 1762 (1986).
31. D. Demus and D. Richter, in: *Textures of Liquid Crystals*, Verlag Chemie, Weinheim, 1978, p. 32.
32. H. R. Allcock, D. C. Ngo, M. Parvez, R. R. Whittle and W. J. Birdsall, *J. Am. Chem. Soc.* **113**, 2628 (1991).